RSC Advances

PAPER

View Article Online
View Journal | View Issue

Cite this: RSC Adv., 2014, 4, 50163

Synthesis and characterization of novel polyimides from 4,4′-bis(5-amino-2-pyridinoxy)diphenyl ether, 4,4′-bis(5-amino-2-pyridinoxy)diphenyl thioether and 4,4′-bis(5-amino-2-pyridinoxy)diphenyl sulfone

Yue Guan,[a] Daming Wang,[a] Zhen Wang,[b] Guodong Dang,[a] Chunhai Chen,[a] Hongwei Zhou[a] and Xiaogang Zhao*[a]

Received 31st July 2014
Accepted 19th September 2014

DOI: 10.1039/c4ra07855a

www.rsc.org/advances

To investigate the difference of the –O–, –SO_2– and –S– groups affecting the thermal, mechanical, optical properties and water uptake of polyimides (PIs), we prepared 4,4′-bis(5-amino-2-pyridinoxy)diphenyl ether (BAPDE), 4,4′-bis(5-amino-2-pyridinoxy)diphenyl sulfone (BAPDS) and 4,4′-bis(5-amino-2-pyridinoxy) diphenyl thioether (BAPDT) with 2-chloro-5-nitropyridine and 4,4′-thiodiphenol, 4,4′-oxydiphenol, 4,4′-sulfonylbisphenol, respectively. Two series of novel PI-(1,3,5) and PI-(2,4,6) were synthesized from BAPDE, BAPDS and BAPDT with two aromatic dianhydrides: 4,4-oxydiphthalic anhydride (ODPA), and 3,3′,4,4′-thiodiphenyl tertracaboxylic dianhydride (TDPA), through a typical two-step polymerization method. The resulting polyimides exhibited solubility in polar solvents, such as DMAc, NMP, DMF, DMSO and *m*-cresol at room temperature. These polyimides with inherent viscosities of 0.84–1.26 dL g^{-1} exhibited high enough molecular weight to give tough and flexible thin films by solution casting. The glass transition temperature (T_g) values measured by differential scanning calorimetric and thermal stabilities based on 5% weight loss temperature of PI films varied from 226 to 305 °C and from 453 to 483 °C, respectively. Interestingly, the influence of oxygen and sulfur-connected ether linkage in diamine and dianhydride on T_g exhibits the reverse order. The polyimides also have good mechanical properties, tensile strengths of 101–114 MPa, tensile modulus of 2.8–3.2 GPa, and elongations at break of 8.8–33.3%. The cutoff wavelengths and transparency of PI films were in the ranges of 338–400 nm and 72–84% at 500 nm, respectively. The water uptakes of the resulting PI films were in the range of 0.5–1.4%.

1 Introduction

Aromatic polyimides (PIs) are well known as high performance polymeric materials for their excellent comprehensive properties, such as high thermal, oxidative, chemical, and mechanical stabilities.[1–5] Incorporation of specific functionality into the polyimide backbones results in various advanced functional materials. Recently, a series of novel aromatic polyimides[6–11] containing –O–, –SO_2– and –S– groups has been developed in an attempt to overcome the disadvantages of conventional polyimides, such as difficulty to process for poor solubility in organic solvents, poor optical properties, thus limiting their applications. Incorporation of oxygen-connected ether linkage into polyimides through diamine or dianhydride can often improve the solubility and increase the transmittance. Sulfone group-containing polyimides exhibit high glass transition temperature (T_g), mechanical strength, and optical transparency. Sulfur-connected ether linkage is more flexible for the existence of a 3d orbit of sulfur atom which was incorporated into polyimides backbone can improve solubility and processability.[12] Meanwhile, sulfur element with a low molar volume and high molar refraction, incorporated into polyimides[13–15] gives a great benefit to enhance the refractive index in polymers for optical applications.

Pyridine is an electron deficient aromatic hetero-cycle having a localized lone pair of electrons in the sp^2 orbital on the nitrogen atom. The C–N=C bond possesses relatively high molar refraction (4.10) compared to a C=C bond (1.73).[16] Consequently, it is just an efficient way that incorporating of pyridine ring into polymer backbones to increase the refractive index and optical transparency while not deteriorating thermal properties. Moreover, the presence of a nitrogen atom in the polymer structure offers a polarized bond which increases dipole–dipole interactions in the polymer solvent system and improves the solubility of the derived polymers.[17] Also, the

[a]Alan G. MacDiarmid Institute of Jilin University, Changchun, 130012, PR China
[b]Polymer Composites Engineering Laboratory, Changchun Institute of Applied Chemistry, Chinese Academy of Sciences, Changchun 130022, People's Republic of China

presence of a nitrogen atom with a free electron in pyridine units, gives an opportunity for protonation to modify optical properties.[18]

In this paper, polymers, containing –O–, –SO_2– and –S– groups and aromatic pyridine hetero-cycles, were designed and synthesized to clarify structure–property relationships. Three novel monomers, 4,4′-bis(5-amino-2-pyridinoxy)diphenyl thioether, 4,4′-bis(5-amino-2-pyridinoxy)diphenyl sulfone and 4,4′-bis(5-amino-2-pyridinoxy)diphenyl ether were synthesized to prepare polyimides with 3,3′,4,4′-oxydiphthalic anhydride (ODPA) and 3,3′,4,4′-thiodiphenyl tertracaboxylic dianhydride (TDPA), respectively. The influences of the molecular structures on the thermal stability, optical transparency, mechanical property, solubility were systematically investigated.

2 Experiments

2.1 Materials

3,3′,4,4′-Oxydiphthalic anhydride (ODPA) was purchased from Sinopharm Chemical Reagent Beijing Co. Ltd, and 3,3′,4,4′-thiodiphenyl tertracaboxylic dianhydride (TDPA) was kindly supplied by Changchun Institute of Applied Chemistry Chinese Academy of Science, and the two aromatic dianhydrides were recrystallized from acetic anhydride and then dried in vacuum at 150 °C for 10 h prior to use. The compounds, 2-chloro-5-nitropyridine, 4,4′-sulfonylbisphenol, 4,4′-oxydiphenol, 4,4′-thiodiphenol, anhydrous potassium carbonate (K_2CO_3), 10% palladium on charcoal (Pd/C), 80% hydrazine monohydrate and $SnCl_2 \cdot 2H_2O$ were all purchased from Acros and used as received. *N*,*N*-Dimethylformamide (DMF) and *N*,*N*-dimethylacetamide (DMAc) were purified by vacuum distillation over CaH_2 and stored over 4 Å Molecular sieves prior to use. The other commercially available reagents and solvents were also used without further purification.

2.2 Measurements

Inherent viscosities (η_{inh}) were measured with an Ubbelohde viscometer with a 0.5 g dL^{-1} of DMAc solution at 25 °C. High-resolution liquid chromatography mass spectrometry (HRLC-MS) data was obtained using Agilent 1290-micrOTOF-QII. Nuclear magnetic resonance (NMR) spectra were determined on a BRUKER-300 spectrometer at 300 MHz for ^1H and 75 MHz for ^{13}C in deuterated dimethyl sulfoxide (DMSO-d_6). Elemental analyses were performed on a Vario EL cube CHN recorder elemental analysis instrument. FT-IR spectra were recorded on a Bruker Vector 22 spectrometer at a resolution of 4 cm^{-1} in the range of 400–4000 cm^{-1}, with the sample form of powder (monomers) and thin films (PIs). Dynamic mechanical analysis (DMA) was carried out with a TA instrument DMA Q800 at a heating rate of 5 °C min^{-1} and a load frequency of 1 Hz in film tension geometry, T_g was regarded as the peak temperature of loss modulus (E''). Differential scanning calorimetric (DSC) analysis was performed on a TA instrument DSC Q100 at a scanning rate of 10 °C min^{-1} in a nitrogen flow of 50 mL min^{-1}. Thermo gravimetric analysis (TGA) was conducted with the TA 2050, with a heating rate of 10 °C min^{-1} under nitrogen atmosphere. Ultraviolet (UV)-visible (Vis) spectra of the films were recorded on a Shimadzu UV-Vis 2501 spectrometer in transmittance mode at room temperature. Mechanical properties of the films were measured at room temperature by a Shimadzu AG-I universal testing apparatus with crosshead speed of 5 mm min^{-1}. Measurements were performed at 25 °C with film specimens (30–50 μm thick, 3 mm wide and 6 cm long) and average of at least five individual determinations was used. Water uptake (WU) of the films was measured by the weight differences before and after immersion in deionized water at room temperature for 72 h, using the following equation:

$$\mathrm{WU} = \frac{W_{\mathrm{wet}} - W_{\mathrm{dry}}}{W_{\mathrm{dry}}} \times 100\%$$

where W_{wet} is the weight of the film samples after immersion in deionized water, and W_{dry} is the initial weight of the samples. The water uptake of the polyimides is the mean data of three parallel samples.

2.3 Monomer synthesis

2.3.1 Synthesis of 4,4′-bis(5-nitro-2-pyridinoxy)diphenyl ether (BNPDE). Under the protection of nitrogen, 2-chloro-5-nitropyridine (6.9 g, 43.5 mmol) and 4,4′-oxydiphenol (4.0 g, 19.8 mmol) were firstly dissolved in 60 mL of freshly distilled DMF in a 100 mL flask with stirring. After the mixture was completely dissolved, anhydrous potassium carbonate (6.0 g, 43.5 mmol) was added. After 30 min of stirring at room temperature, the mixture was continuously reacted at 70 °C for 6 h. Then, the obtained mixture was cooled to room temperature and poured into 500 mL of distilled water. The crude product was collected by filtration, washed with water, and dried in vacuum at 80 °C for overnight. After recrystallization from DMF/water, 7.8 g was obtained (88%). Melting point: 133 °C (DSC peak). FT-IR (KBr): 1608, 1579, 1517, 1495, 1390, 1279, 1235, 1117 cm^{-1}; ^1H NMR (DMSO-d_6, ppm): 9.04 (d, 1H), 8.62 (dd, 1H), 7.29 (d, 2H), 7.26 (d, 1H), 7.20–7.11 (m, 2H); ^{13}C NMR (DMSO-d_6, ppm): 166.83, 154.59, 148.75, 145.10, 140.93, 136.20, 123.69, 120.31, 112.08; HRLC-MS (ESI): 447.3 $(M + H)^+$, calcd 446.4 for $C_{22}H_{14}N_4O_7$.

2.3.2 Synthesis of 4,4′-bis(5-nitro-2-pyridinoxy)diphenyl sulfone(BNPDS). Similarly, BNPDS (yield: 92%) was prepared by the aforementioned procedure. Melting point: 181 °C (DSC peak). FT-IR (KBr): 1607, 1574, 1520, 1462, 1392, 1264, 1199, 1105 cm^{-1}; ^1H NMR (DMSO-d_6, ppm): 9.04 (dd, 1H), 8.73–8.61 (m, 1H), 8.19–8.07 (m, 2H), 7.59–7.48 (m, 2H), 7.40 (dd, 1H); ^{13}C NMR (DMSO-d_6, ppm): 165.79, 157.19, 144.98, 141.52, 138.46, 136.60, 130.25, 123.40, 112.93; HRLC-MS (ESI): 495.3 $(M + H)^+$, calcd 494.4 for $C_{22}H_{14}N_4O_8S$.

2.3.3 Synthesis of 4,4′-bis(5-nitro-2-pyridinoxy)diphenyl thioether(BNPDT). Similarly, BNPDT (yield: 86%) was prepared by the aforementioned procedure. Melting point: 136 °C (DSC peak). FT-IR (KBr): 1607, 1574, 1516, 1486, 1387, 1261, 1195, 1116 cm^{-1}; ^1H NMR (DMSO-d_6, ppm): 9.03 (t, 1H), 8.62 (dd, 1H), 7.50–7.45 (m, 2H), 7.30 (s, 1H), 7.28 (dd, 2H); ^{13}C NMR (DMSO-d_6, ppm): 166.43, 152.67, 145.04, 141.08, 136.30,

132.97, 132.20, 123.35, 112.36; HRLC-MS (ESI): 463.3 $(M + H)^+$, calcd 462.4 for $C_{22}H_{14}N_4O_6S$.

2.3.4 Synthesis of 4,4′-bis(5-amino-2-pyridinoxy)diphenyl ether(BAPDE). Under the protection of nitrogen, 4.5 g (10.1 mmol) of BNPDE, 0.7 g of palladium on activated carbon (Pd/C 10%), and 100 mL of dioxane were added to a 250 mL three-necked flask equipped with a dropping funnel, and a reflux condenser. After heating to refluxing temperature with stirring, 20 mL of hydrazine monohydrate was added dropwise in 1 h. Then, the mixture was heated at refluxing temperature for additional 6 h. The mixture was filtered and the filtrate was subsequently concentrated and poured into 500 mL of water to produce a precipitate, which was collected by filtration, washed with water. After recrystallization from dioxane/water, the product was dried at 60 °C under vacuum for overnight, and 3.3 g of BAPDE was obtained (85%). Melting point: 155 °C (DSC peak). FT-IR (KBr): 3392, 3315, 1637, 1581, 1476, 1419, 1278, 1244, 1190, 1095 cm^{-1}; ^1H NMR (DMSO-d_6, ppm): 7.56 (d, 1H), 7.09 (dd, 1H), 7.01–6.96 (m, 4H), 6.76 (d, 1H), 5.06 (s, 2H); ^{13}C NMR (DMSO-d_6, ppm): 154.35, 152.94, 152.04, 142.25, 132.71, 125.89, 121.14, 119.89, 112.86; HRLC-MS (ESI): 387.3 $(M + H)^+$, calcd 386.4 for $C_{22}H_{14}N_4O_3$.

2.3.5 Synthesis of 4,4′-bis(5-amino-2-pyridinoxy)diphenyl sulfone(BAPDS). Similarly, BAPDS (yield: 93%) was prepared by the same procedure as BAPDE (recrystallization from dioxane/water). Melting point: 148 °C (DSC peak). FT-IR (KBr): 3413, 3358, 1631, 1584, 1477, 1416, 1241, 1150, 1105 cm^{-1}; ^1H NMR (DMSO-d_6, ppm): 7.99–7.77 (m, 2H), 7.60 (t, 1H), 7.12 (dd, 2H), 7.09 (t, 1H), 6.87 (d, 1H), 5.28 (s, 2H); ^{13}C NMR (DMSO-d_6, ppm): 161.01, 152.17, 143.52, 135.54, 133.06, 129.86, 125.61, 119.19, 114.30; HRLC-MS (ESI): 435.4 $(M + H)^+$, calcd 434.5 for $C_{22}H_{18}N_4O_4S$.

2.3.6 Synthesis of 4,4′-bis(5-amino-2-pyridinoxy)diphenyl thioether (BAPDT). Under nitrogen protection, 6.0 g (12.9 mmol) of BNPDT, 29.1 g (129.0 mmol) of $SnCl_2 \cdot 2H_2O$ was charged into a reaction flask, while 47 mL of concentrated hydrochloric acid was added slowly. After addition of hydrochloric acid was finished, the mixture was refluxed for 7 h. The reaction mixture was cooled to room temperature and poured into 400 mL of distiller water, the mixing solution was basified with 20% NaOH solution to form a precipitate, and the precipitate was filtrated off, washing with water, recrystallized from ethanol to get a white product. After dried under vacuum at 40 °C for overnight, 1.88 g of BAPDT was obtained (68%). Melting point: 142 °C (DSC peak). FT-IR (KBr): 3397, 3311, 1641, 1585, 1476, 1421, 1275, 1240, 1162, 1084 cm^{-1}; ^1H NMR (DMSO-d_6, ppm): 7.58 (t, 1H), 7.37–7.26 (m, 2H), 7.16–7.05 (m, 1H), 7.00–6.90 (m, 2H), 6.81 (t, 1H), 5.16 (s, 2H); ^{13}C NMR (DMSO-d_6, ppm): 155.85, 152.89, 142.24, 132.34, 128.61, 125.23, 119.77, 113.04, 92.18; HRLC-MS (ESI): 403.4 $(M + H)^+$, calcd 402.5 for $C_{22}H_{18}N_4O_2S$.

2.4 Polymer synthesis

The polyimides were synthesized by the conventional two-step procedure *via* poly(amic acid) precursors, followed by thermally curing at elevated temperatures, as shown in Scheme 2. The synthesis of polyimide PI-1 (ODPA/BAPDE) is employed as an example to illustrate the general synthetic route. 1.0857 g ODPA (3.5 mmol) was added to a solution of 1.3524 g BAPDE (3.5 mmol) in 9.75 g DMAc in two portions. Extra 4.07 g DMAc was added to adjust the solid content of the reaction system to 15% by weight. The mixture was stirred at room temperature for 24 h to afford a viscous poly(amic acid) solution.

PI films were prepared by thermal imidization of PAA solutions cast onto glass plates, followed by a preheating program (60 °C/1 h, 80 °C/3 h, 120 °C/1 h) and an imidization procedure under vacuum (250 °C/1 h, and 300 °C/1 h) to produce a fully imidized polyimide film. Polyimide film was stripped from the glass substrate by immersing the glass plate in hot deionized water. The thickness of PIs films was controlled to be about 10 μm for UV-vis and FT-IR measurements and the specimen for thermal and mechanical properties measurements was adjusted to be 30–50 μm.

PI-2 (TDPA/BAPDE), PI-3 (ODPA/BAPDS), PI-4 (TDPA/BAPDS), PI-5 (ODPA/BAPDT) and PI-6 (TDPA/BAPDT) were synthesized by the similar method described above.

3 Result and discussion

3.1 Monomer synthesis

The synthetic route of new diamine monomers was outlined in Scheme 1. Three dinitro compounds, BNPDT, BNPDS, and BNPDE were prepared by a nucleophilic chloro-displacement reaction of 2-chloro-5-nitropyridine with 4,4′-thiodiphenol, 4,4′-sulfonylbisphenol, 4,4′-oxydiphenol in the presence of anhydrous potassium carbonate in DMF, respectively. Owing to the presence of an electronegative nitrogen atom in the aromatic ring, pyridine derivatives undergo nucleophilic substitution much more easily than the corresponding benzenes, especially at the 2- and 4- positions.[19] Moreover, the para nitro-group activated the chlorine atom for displacement. Therefore, the chlorine-displacement reaction of 2-chloro-5-nitropyridine by the phenoxide anion was readily carried out. BNPDS and BNPDE were reduced by Pd/C and 80% $NH_2NH_2 \cdot H_2O$ in dioxane at refluxing temperature for several hours in high yields. BNPDT was converted to BAPDT by reduced with $SnCl_2 \cdot 2H_2O$ and concentrated hydrochloric acid at refluxing

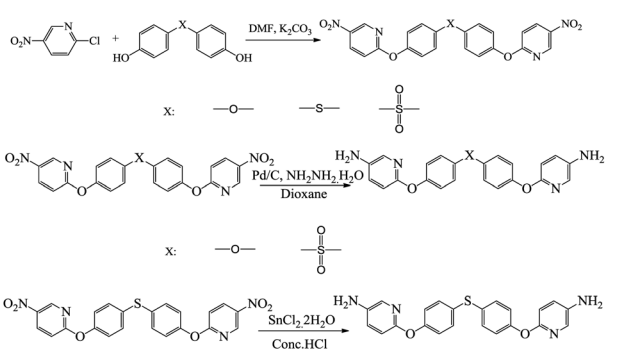

Scheme 1 Synthesis of the monomers.

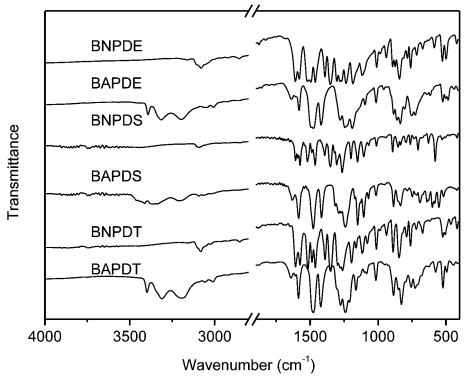

Fig. 1 FT-IR spectra of dinitro intermediates and diamine monomers (KBr sample).

temperature. All the diamine monomers and dinitro intermediates were characterized by FT-IR, NMR and HRLC-MS.

Fig. 1 shows the FT-IR spectra of dinitro compounds, BNPDE, BNPDS, BNPDT and diamine, BAPDE, BAPDS, BAPDT. The nitro group of BNPDE, BNPDS, BNPDT gave two characteristic bands at 1517, 1520, 1516 and 1390, 1392, 1387 cm^{-1} ($-NO_2$ asymmetric and symmetric stretching), respectively. After the reduction, the characteristic absorptions of the nitro group disappeared, and the amino group showed a pair of N–H stretching bands in the region of 3310–3450 cm^{-1}. As shown in Fig. 2, ^1H NMR spectra of the diamine monomers illustrate that the nitro groups in BNPDE, BNPDS, BNPDT were completely reduced, in which the signal of amino groups appeared at around δ 5.06, 5.28, 5.16 as a singlet; signals derived from the pyridine ring and the benzene ring appeared good distribution. In ^{13}C NMR spectra, carbon 13 atoms in BAPDE, BAPDS, BAPDT showed clear 9 signals which resonated in the regions of 90–165 ppm. All the spectroscopic data obtained agreed with the expected structures.

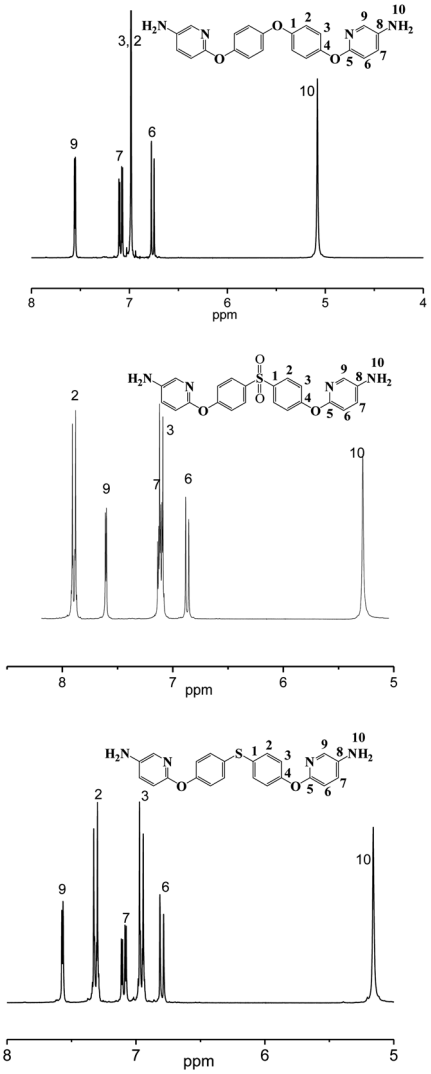

Fig. 2 ^1H NMR spectra of BAPDE, BAPDS and BAPDT monomers.

3.2 Polymer synthesis

The diamine monomers, BAPDE, BAPDS and BAPDT were reacted with two aromatic dianhydrides, ODPA, TDPA respectively, to give the corresponding polyimides, as shown in Scheme 2. The novel polyimides were synthesized using two-step methods, which were carried out *via* poly(amic acid)s (PAA) intermediate. The polymerization was carried out by reacting equimolar amounts of diamine monomer with aromatic dianhydride at a concentration of 15% solids in DMAc. The polycondensation reaction was prepared at room temperature for 24 h yielded PAA (Scheme 2). As shown in Table 2, the inherent viscosities of the PAA precursors were 0.84–1.26 dL g^{-1} in DMAc at 25 °C, indicating that the polymers with relatively high molecular weights were obtained. Tough and flexible polyimide films were obtained by casting the PAA solutions on glass plate followed by thermally curing process at 300 °C.

Chemical structures of the polyimides were characterized with FT-IR. Fig. 3 demonstrates FT-IR spectra of polyimides. All the polyimides exhibited characteristic imide group absorptions around 1780 cm^{-1} (asymmetrical C=O stretching), 1730 cm^{-1} (symmetrical C=O stretching), 1390 cm^{-1} (C–N stretching), and together with some strong absorption bands in the region of 1200–1100 cm^{-1} (C–O stretching). There was no existence of the characteristic absorption bands of the amide group near 3310–3450 cm^{-1} (N–H stretching), which indicated polymers had been fully imidized. The results of the elemental analyses of all the thermally cured polyimides were listed in Table 1. The values found were in good agreement with the calculated ones of the proposed structures.

3.3 Thermal properties

Thermal properties of the polyimides were determined by DSC, DMA and TGA, and the results were listed in Table 2. Glass transition temperatures (T_g) of the polyimides were in the range of 226–305 and 219–260 °C, as obtained by DSC in Fig. 4 and DMA in Fig. 5, respectively. In DMA, T_g was regarded as the peak temperature of loss modulus (E''). The differences of T_g values obtained by DSC and DMA were mainly attributed to the different responses of the samples to the two characterization

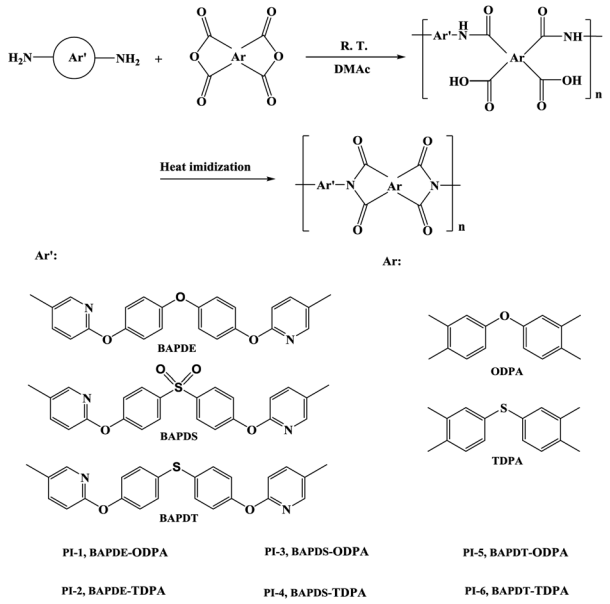

Scheme 2 Synthesis route of the polyimides.

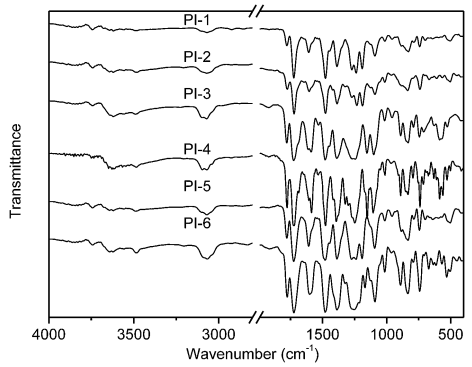

Fig. 3 FT-IR spectra of the PI films.

methods. Generally, T_g values of polymers are determined by molecular packing and chain rigidity of the polymer backbones. As a result, PI-3 and PI-4 based on the most rigid polymer backbone containing –SO_2– group exhibited the higher T_g. Interestingly, in DSC with the same diamine BAPDE, when the thioether linkage is in dianhydride, PI-1 derived from ODPA/BAPDE shows the higher T_g (230 °C) value than that (226 °C) of PI-2 derived from TDPA/BAPDE, and PI-3 (ODPA/BAPDS), PI-4 (TDPA/BAPDS) and PI-5 (ODPA/BAPDT), PI-6 (TDPA/BAPDT) possess the same phenomenon, but with the same dianhydride ODPA, when the thioether linkage is in diamine, PI-5 derived from ODPA/BAPDT shows the slightly higher T_g (232 °C) value than that (230 °C) of PI-1 derived from ODPA/BAPDE, and with the same dianhydride TDPA, PI-6 (TDPA/BAPDT), PI-2 (TDPA/BAPDE) also exhibit the same phenomenon. The T_gs measured by DMA shows the same order. Fig. 5 shows variations in the storage and loss modulus at different temperature in DMA. As shown in Fig. 5, the storage modulus retained constant or decreased slightly before the corresponding T_gs. Regarding the peak temperature in loss modulus as the glass transition temperatures (T_g), the T_g measured by DMA shows the same trends with DSC measurements.

Thermal stabilities of the PIs were evaluated by TGA in nitrogen atmosphere. TGA curves for polyimides were reproduced in Fig. 6. The decomposition temperatures at 5% and 10% weight loss in nitrogen atmospheres were determined from the original TGA thermo-grams and were also given in Table 2. 5% weight loss temperatures (T5%) of the polymers in nitrogen were recorded in the range of 453–487 °C. Furthermore, the residual weight at 800 °C was in the range of 48.7–54.9%. In contrast, as shown in Table 2, with the same diamine, the 5% and 10% weight loss temperature in nitrogen show PI-2 < PI-1, PI-4 < PI-3, PI-6 < PI-5, and with the same dianhydride, 5% and 10% weight loss temperature in nitrogen show PI-1 < PI-5, PI-2=< PI-6. All the TGA results indicated that the obtained polyimides PI-(1–6) possessed excellent thermal stability.

3.4 Optical properties and X-ray diffraction of PI films

The optical transparency of polyimide films were measured by UV-visible spectroscopy. The UV-vis spectra of the PI films with thicknesses of approximately 10 μm were shown in Fig. 7, and the optical data are summarized in Table 3. All the polyimide films exhibit good transparency with the cut-off wavelengths ($\lambda_{cut\text{-}off}$) of 338–400 nm and the transmittances of 72–84% at 500 nm, as shown in Fig. 7. These indicate that pyridine units do not deteriorate the optical transparency. All the films exhibit much better optical transparency than that of the standard aromatic PI, derived from pyromellitic dianhydride (PMDA) and 4,4′-oxydianiline (ODA) to the similar thickness.[20] It can be observed from Fig. 7 that PI derived from ODPA exhibits lower $\lambda_{cut\text{-}off}$ and higher transparency than PI derived from TDPA, when the

Table 1 Elemental analysis of the polyimides

PIs	Formula of repeating unit	Elemental analysis (%)				
			C	H	N	O
PI-1	$C_{38}H_{20}N_4O_8$	Calcd found	69.09 68.58	3.05 3.14	8.48 8.44	19.38 19.80
PI-2	$C_{38}H_{20}N_4O_7S$	Calcd found	67.45 67.02	2.98 3.04	8.28 8.21	16.55 16.74
PI-3	$C_{38}H_{20}N_4O_9S$	Calcd found	64.40 63.62	2.84 2.82	7.91 7.83	20.32 20.46
PI-4	$C_{38}H_{20}N_4O_8S_2$	Calcd found	62.98 62.26	2.78 2.49	7.73 7.66	17.66 17.98
PI-5	$C_{38}H_{20}N_4O_7S$	Calcd found	67.45 66.72	2.98 2.65	8.28 8.29	16.55 16.88
PI-6	$C_{38}H_{20}N_4O_6S_2$	Calcd found	65.89 65.25	2.91 2.56	8.09 7.99	13.86 13.92

Table 2 Physical properties and thermal properties of the PI films[a]

PIs	η_{inh} of PAA[b] (dL g^{-1})	T_g (°C) DSC[c]	T_g (°C) DMA[d]	T5%[e] (°C)	T10%[e] (°C)	Rw[f] (%)
PI-1	1.26	230	229	477	500	54.9
PI-2	1.18	226	224	465	488	54.6
PI-3	0.84	305	260	471	495	49.2
PI-4	0.86	295	259	453	480	47.6
PI-5	1.12	232	222	487	505	53.4
PI-6	1.08	227	219	465	489	48.7

[a] η_{inh}: inherent viscosities; T_g: glass transition temperature; T5%: 5% weight loss temperature; T10%: 10% weight loss temperature; Rw: residual weight; DSC: differential scanning calorimetry; DMA: dynamic mechanical analysis; TGA: thermogravimetric analysis; N_2: nitrogen. [b] Measured at polymer concentration of 0.5 g dL^{-1} in DMAc at 25 °C. [c] Obtained at the baseline shift in the second heating DSC traces at a heating rate of 10 °C min^{-1} under N_2 atmosphere. [d] Obtained at a heating rate of 5 °C min^{-1} and a load frequency of 1 Hz in film tension geometry. [e] Obtained by TGA at a heating rate of 10 °C min^{-1} under N_2 atmosphere. [f] Obtained at 800 °C by TGA at a heating rate of 10 °C min^{-1} under N_2 atmosphere.

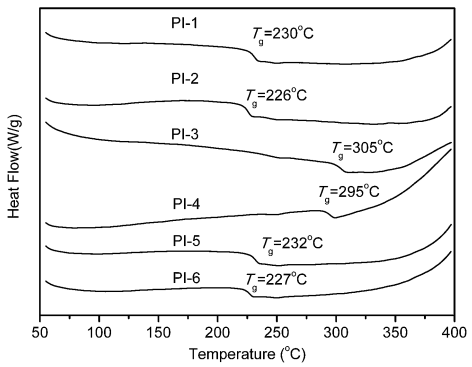

Fig. 4 DSC curves of the polyimide films.

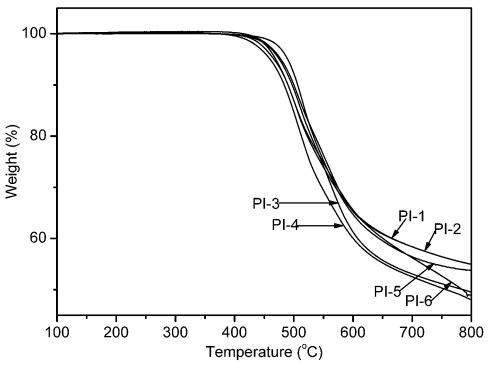

Fig. 6 TGA curves of the polyimides.

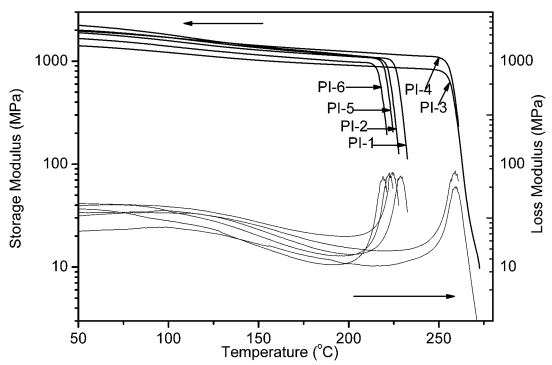

Fig. 5 The storage and loss modulus curves of the PI films in DMA.

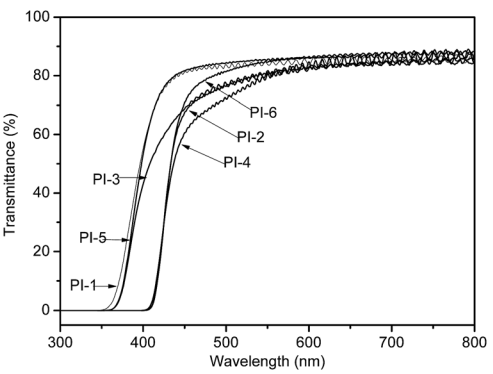

Fig. 7 UV-visible spectra of the PI films.

diamine structures are fixed. According to the CTC theory, PI-1 derived from ODPA and BAPDE containing more –O– linkage in the polymer backbone shows the shortest $\lambda_{cut\text{-}off}$ and the highest transparency at 500 nm. Meanwhile, PI-1 derived from ODPA and BAPDE exhibits the higher transparency and lower $\lambda_{cut\text{-}off}$ than that of PI-3 derived from ODPA and BAPDS, which comply with the order reported by S. Ando.[21]

The morphological structure of the polyimides was analyzed by wide-angle X-ray diffraction analysis, 2θ ranging from 5 to 50°, using the polyimide films as samples, and the results were shown in Fig. 8. The X-ray diffraction curves of the polyimides express a set of wider diffraction peak, and these should be evidences that indicate the polyimides holding morphology, which is attributed to the incorporation of flexible ether or thioether linkage loosening the chain packing of the polymer and the pyridyl ether linkage units having the twist polymer backbone structure.[22]

3.5 Mechanical properties and water uptake of PI films

All of the polyimides could be processed into good quality, freestanding films. These films were subjected to tensile tests.

Table 3 Mechanical properties of PI films[a]

PIs	T_S (MPa)	T_M (GPa)	E_B (%)	$\lambda_{cut\text{-}off}$[b] (nm)	Transmittance[c] (%)	WU[d] (%)
PI-1	110 ± 1.8[e]	2.9 ± 0.21	33.3 ± 0.5	338	84	0.9
PI-2	108 ± 2.6	2.8 ± 0.20	28.5 ± 0.3	400	76	1.2
PI-3	114 ± 2.4	2.9 ± 0.18	11.6 ± 0.2	354	77	1.0
PI-4	112 ± 1.3	3.0 ± 0.13	8.8 ± 0.6	398	72	1.4
PI-5	109 ± 3.0	3.2 ± 0.12	17.8 ± 0.5	354	84	0.5
PI-6	101 ± 3.2	2.9 ± 0.22	13.2 ± 0.3	399	81	1.0

[a] T_S, tensile strength; T_M, tensile modulus; E_B, elongation at break. [b] Cutoff wavelength. [c] Transmittance at 500 nm. [d] Water uptake. [e] 1.8, standard deviation.

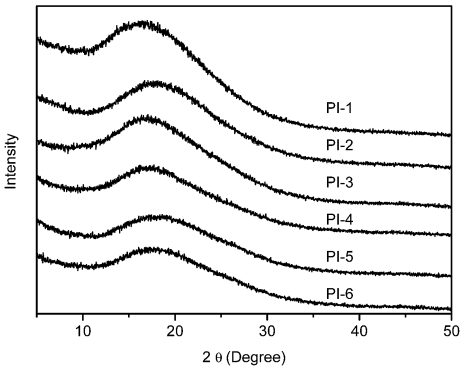

Fig. 8 Wide-angle X-ray diffraction curves of the polyimide films.

Table 4 Solubility behavior of the polyimides[ab]

Solvents	PI-1	PI-2	PI-3	PI-4	PI-5	PI-6
m-Cresol	+−	+−	+−	+−	+−	+−
DMF	+−	+−	+−	+−	+−	+−
DMAc	++	++	+−	+−	++	++
NMP	++	++	+−	+−	++	++
DMSO	+−	+−	+−	+−	+−	+−
THF	−−	−−	−−	−−	−−	−−
$CHCl_3$	−−	−−	−−	−−	−−	−−
Cyclohexanone	−−	−−	−−	−−	−−	−−
CH_3COOH	−−	−−	−−	−−	−−	−−
Pyridine	+−	+−	−−	−−	+−	+−

[a] Solubility was determined with 10 mg of polyimides in 1 mL of solvent at room temperature for 72 h. [b] ++, soluble at room temperature; +−, partial soluble; −−, insoluble.

Table 3 shows the mechanical properties of the polyimides, including the tensile strength (T_S), tensile modulus (T_M) as well as elongation at break (E_B). Polyimide films exhibited good mechanical properties with tensile strength of 101–114 MPa, tensile moduli of 2.8–3.2 GPa and elongations at breakage of 8.8–33.3%. The elongation at break of polyimides were followed an order of PI-1 > PI-5 > PI-3 and PI-2 > PI-6 > PI-4, where the dianhydride structures was fixed. It might be due to the increase in chain flexibility with the existence of more ether bond groups. PI-3 and PI-4 containing rigid –SO_2– group exhibit the higher tensile strength and the lower elongation at break. Tensile strength of PI derived from ODPA was similarity or slightly higher than that of PI derived from TDPA, where the dianmine structures were fixed. It might be explained by the rigid of –O– group was higher than that of –S– group.[12]

The water uptake of the polyimides is the mean data of three parallel samples which showed in the range of 0.5–1.4% at room temperature for 72 h (Table 3). Water uptake (0.51%) of PI-5 film was very similar to that (0.52%) of Kapton film[23] and water absorption rate of Upilex®-75S was measured to be 1.49% under the same conditions. These results implied that introduction of pyridine moiety did not deteriorate the water absorption of the polyimides.

3.6 Solubility of the polyimide films

The solubility of the PI films was determined by dissolving 10 mg of polymers in 1 mL of solvent at room temperature, and the results were listed in Table 4. The polyimide PI (1–6) showed certain solubility in polar solvents, such as DMAc, NMP, DMF, DMSO and *m*-cresol at room temperature. The solubility should result from the introduction of the flexible ether or thioether groups in the polymer backbone, which decreased the interaction between polymer chains and chain symmetry, leading to amorphous morphology, which in turn increases solubility. Meanwhile, the presence of pyridine ring nitrogen atom in the structure produces a polarized bond and increases dipole–dipole interactions in the polymer-solvent system which gives a benefit to improve the solubility of the prepared polymers.[17] As shown in Table 4, the PI-1, PI-2, PI-5, PI-6 exhibited the better solubility than PI-3 and PI-4, which might be attributed to more ether or thioether linkage in the polymer backbone.

4 Conclusions

Three novel aromatic diamines were designed and synthesized, which were employed to react with two aromatic dianhydrides, ODPA and TDPA to yield two series of polyimides, through a typical two-step polymerization method. The performance data of the resulting polyimides was comprehensively tested and these polyimides exhibited solubility in polar solvents, fantastic optical properties, high thermal stability, and excellent mechanical property. Especially, we find the reverse influence of –O– and –S– groups in diamine and dianhydride on glass transition temperature of the polyimides. In addition, through clarifying the structure–property relationship of the obtained

polyimides derived from the analogous monomers, BAPDE, BAPDS, and BAPDT, it is a great benefit to design novel structure monomers using –O–, –S–, –SO_2– groups for improving thermal, optical and exceptional property.

Acknowledgements

Financial support by the National Nature Science Foundation of China (National 973 program no. G2010CB631100) and the National Technology Support Program (no. 2011BAA06B03) are gratefully acknowledged.

Notes and references

1 C. E. Sroog, History of the Invention and Development of the Polyimides, in *Polyimides fundamentals and applications*, ed. M. K. Ghosh and K. L. Mittal, Marcel Dekker, New York, 1996, pp. 1–6.
2 K. L. Mittal, *Polyimides and Other High-temperature polymers*, VSP/Brill, Leiden, The Netherlands, 2009.
3 *Polyimides*, ed. M. I. Bessonov, M. M. Koton, V. V. Kudryavtsev and L. A. Laius, Consultants Bureau, New York, NY, 1987.
4 *Polyimides*, ed. M. K. Ghosh and K. L. Mittal, Marcel Dekker, New York, 1996.
5 T. Takekoshi, *Encyclopedia of Chemical Technology*, ed. Kirkother, Wiley, New York, 1996, vol. 19, pp. 813–37.
6 W. B. Jang, D. Y. Shin, S. H. Choi, S. G. Park and H. Han, *Polymer*, 2007, **48**, 2130.
7 Y. Han, X. Z. Fang and X. X. Zuo, *J. Mater. Sci.*, 2010, **45**, 1921.
8 M. X. Ding, H. Y. Li, Z. H. Yang, Y. S. Li, J. Zhang and X. Q. Wang, *J. Appl. Polym. Sci.*, 1996, **59**, 923.
9 H. B. Wei, X. L. Pei and X. Z. Fang, *J. Polym. Sci., Part A: Polym. Chem.*, 2011, **49**, 2484.
10 M. Chao, K. C. Kou, G. L. Wu and D. N. Zhang, *J. Macromol. Sci., Part A: Pure Appl.Chem.*, 2012, **49**, 578.
11 P. Thiruvasagam and D. Venkatesan, *High Perform. Polym.*, 2011, **23**, 22.
12 F. Liu, Z. Wang, H. L. Yang, L. X. Gao and M. X. Ding, *Polymer*, 2006, **47**, 937.
13 N. H. You, T. Higashihara, S. Ando and M. Ueda, *J. Polym. Sci., Part A: Polym. Chem.*, 2010, **48**, 656.
14 J. G. Liu, Y. Nakamura, Y. Shibasaki, S. Ando and M. Ueda, *Macromolecules*, 2007, **40**, 4614.
15 N. H. You, Y. Suzuki, D. Yorifuji, S. Ando and M. Ueda, *Macromolecules*, 2008, **41**, 6361.
16 J. G. Speight, *Lange's hand book of chemistry*, 16th edn, McGraw-Hill, 2005.
17 S. J. Zhang, Y. F. Li, X. L. Wang, X. Zhao, Y. Shao, D. X. Yin and S. Y. Yang, *Polymer*, 2005, **46**, 11986.
18 E. Grabiec, M. Kurcok and E. Schab-Balcerzak, *J. Phys. Chem. A*, 2009, **113**, 1481.
19 A. A. El-Bardan, *J. Phys. Org. Chem.*, 1999, **12**, 347.
20 J. G. Liu, Y. Nakamura, Y. Shibasaki, S. Ando and M. Ueda, *J. Polym. Sci., Part A: Polym. Chem.*, 2007, **45**, 5606.
21 S. Ando, T. Matsuura and S. Sasaki, *Polym. J.*, 1997, **29**, 69.
22 I. In and S. Y. Kim, *Polymer*, 2006, **47**, 547.
23 C. P. Yang, R. S. Chen and K. H. Chen, *J. Polym. Sci., Part A: Polym. Chem.*, 2003, **41**, 922.

